The Japan Society of Mechanical Engineers

Stress Intensity Factors of a Subsurface Crack in a Semi-Infinite Body due to Rolling/Sliding Contact and Heat Generation*

Takahito GOSHIMA** and Toshimichi SODA***

This paper deals with the two-dimensional thermoelastic contact problem of a rolling rigid cylinder of specified shape, which induces of friction and heat generation in the contact region, moving with constant velocity in an elastic half-space containing a subsurface crack. In the present temperature analysis, the speed of the moving heat source is assumed to be much greater than the ratio of the thermal diffusivity and the contact length. The problem is solved using complex-variable techniques and is reduced to singular integral equations which are solved numerically. Numerical results of stress intensity factors are obtained for a relatively short crack. The effects of the frictional coefficient, the sliding/rolling ratio, the crack depth and the crack angle on the stress intensity factors are considered.

Key Words: Elasticity, Thermal Stress, Stress Intensity Factor Subsurface Crack, Rolling/Sliding Contact, Frictional Heating

1. Introduction

The rolling contact fatigue failure, such as shelling in railroads, spalling in rollers, may be manifested by originating and growing subsurface crack due to periodic rolling/sliding contact. These subsurface cracks may be initiated by preexisting defects such as inclusions, gas pores, or local soft spots, or may be generated during the cyclic straining process itself. Since the analysis for delamination theory of Suh[1], a considerable amount of research[2]-[8] on fracture mechanics has been performed in order to understand the mechanism of subsurface crack initiation and propagation in rolling/sliding contacts. These studies, however, dealt with an isothermal case. Most rolling contacts are accompanied by frictional heat generation due to the relative slip between the two contact surfaces. Goshima and coworkers[9]-[14] subsequently dealt with the thermoelastic rolling contact problem for a inclined surface crack. In these studies, it was impossible to calculate for the shallow crack of the inclination angle being under 20° in connection with the tribological failure such as shelling. However, for the analysis of the actual rolling contact fatigue failure such as shelling or spalling, the subsurface crack model is profitable. For the analysis of a subsurface crack accompanied by frictional heating, Chen et al.[15] has delt with a near-surface horizontal line crack with the moving frictional heating. Although this study was delt with as a thermoelastic problem, they do not consider the rolling/sliding contact from mechanical standpoint. The subsurface crack analysis under rolling/sliding contact accompanied by frictional heating has not been performed as yet.

In this study, we analyze the stress intensity factors for a subsurface crack in an elastic half-space under rolling/sliding contact accompanied by frictional heating. This thermoelastic contact is dealt with as a mixed boundary value problem with a specified displacement shape beneath the rigid roller. The crack face friction is neglected. In the present

* Received 17th March, 1997. Japanese original: Trans. Jpn. Soc. Mech. Eng., Vol. 62, No. 600, A (1996), p. 1854-1861 (Received 8th November, 1995)

** Faculty of Engineering, Toyama University, 3190 Gofuku, Toyama-City 930, Japan

*** Aichi Steel Corporation, 1 Wano Wari Arao-Machi, Toukai-City 476, Japan

NII-Electronic Library Service

The Japan Society of Mechanical Engineers

temperature analysis, it is assumed that the speed of the moving contact region is much greater than the ratio of the thermal diffusivity to the contact length (large Peclet number), and that the temperature distribution is not disturbed by the crack. Numerical calculations of stress intensity factors are carried out for a short crack. The effects of the frictional coefficient, the slide/roll ratio and the crack depth and the crack angle upon the stress intensity factors are considered numerically.

2. Problem Formulation

An elastic half-space containing a subsurface crack is subjected to rolling/sliding contact by a rigid roller with constant moving velocity V, as shown in Fig. 1. The surface of the half-space is specified as the displacement shape of the roller in the contact region. In the analysis, the following dimensionless parameters are used.

$$(x, y)=(\tilde{x}/c, \tilde{y}/c),\ (\xi, \zeta)=(\tilde{\xi}/c, \tilde{\zeta}/c)$$
$$x_1=\tilde{x}_1/c,\ y_1=\tilde{y}_1/c,\ x_0=\tilde{x}_0/c,\ y_0=\tilde{y}_0/c$$
$$R=\tilde{R}/c,\ \iota=\tilde{\iota}/c,\ P_e=cV/\kappa_t,\ S_r=V_s/V$$
$$H_0=\frac{2\alpha_0 G_0 \kappa_t(1+\nu)}{K_t(1-\nu)},\ P_r=\frac{RP_0}{G_0}$$

where, κ_t is thermal diffusivity, K_t is thermal conductivity, G_0 is shear modulus, ν is Poisson's ratio, α_0 is coefficient of thermal expansion, P_0 is the maximum pressure, $\tilde{x}_0$ and $\tilde{y}_0$ are the rigid displacement components of the roller, V_s is the sliding velocity during rolling contact, P_e is Peclet number and S_r is the slide/roll ratio.

Assuming that all the work done by the friction load is transformed into heat energy, the frictional-heat generation is given as $Q_1(x)=fV_sP_1(x)$, $P_1(x)$ being contact pressure and f being frictional coefficient. However in the present study, having specified the displacement shape of the roller, the contact pressure distribution $P_1(x)$ is not given, and $Q_1(x)$ cannot be determined. In the present analysis,

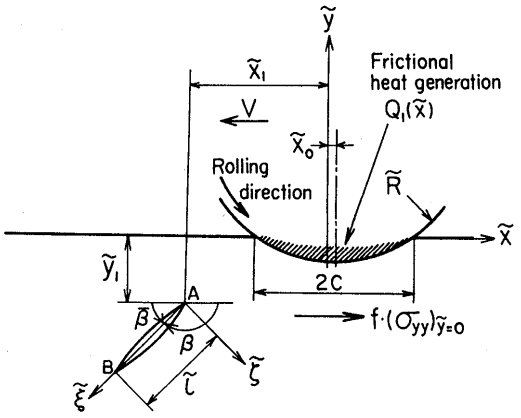

Fig. 1 Problem configuration and coordinate system

we assume that the frictional heat generation $Q_1(x)$ is given as

$$Q_1(x)=Q_0Q(x)=fVS_rP_0Q(x), \quad (1)$$

where the distribution of heat generation $Q(x)$ is assumed to be a proper function of x.

The region outside the area of contact is assumed to be thermally insulated. Furthermore, it is assumed that the temperature distribution $T(x, y)$ is not affected by the presence of crack. Thus, the thermal boundary conditions can be given as follows.

$$\left(\frac{\partial T}{\partial y}\right)_{y=0}=\begin{cases} fcVS_rP_0Q(x)/K_t, & |x|<1 \\ 0, & |x|>1 \end{cases} \quad (2)$$

$$(T)_{y\to-\infty}=0 \quad (3)$$

The mechanical boundary conditions on the surface and at infinity of the half-space are given as

$$\sigma_{xy}+f\sigma_{yy}=0, \quad |x|<1 \quad (4)$$
$$\sigma_{yy}+i\sigma_{xy}=0, \quad |x|>1 \quad (5)$$
$$U'_{yy}/c=(x-x_0)^2/(2R)+y_0, \quad |x|<1 \quad (6)$$
$$(\sigma_{pq})_{y\to-\infty}=0, \ (p, q=x, y), \quad (7)$$

where $\sigma_{pq}(p, q=x, y)$ are the stress components, U_{yy} is a vertical displacement and $i^2=-1$.

Assuming that crack-face friction is neglected, the boundary condition along the crack may be expressed as

$$(\sigma_{\xi_k\zeta_k})_{\zeta_k=0}=0, \ 0<\xi_k<\iota_k, \ k=1, 2 \quad (8)$$
$$(\sigma_{\zeta_k\zeta_k})_{\zeta_k=0}=0, \ \xi_k\in\xi_{kop}, \ k=1, 2, \quad (9)$$

where ξ_{kop} is the crack face opening region of the crack.

We require continuity of displacements throughout the body except at the crack and hence the condition for single-valued of displacements is shown as

$$\oint(U_{xx}+iU_{yy})dz=0, \ (z=x+iy) \quad (10)$$

where $\oint$ denotes the integration along a contour around the subsurface crack.

3. Stress Analysis

In general, using Muskhelishivili's complex stress function $\Phi(z)$, $\Psi(z)$ and a thermoelastic potential ω, thermal stresses and displacements are represented as[16].

$$\sigma_{yy}+\sigma_{xx}=2\{\Phi(z)+\overline{\Phi(z)}\}-2G_0\nabla^2\omega \quad (11)$$
$$\sigma_{yy}-\sigma_{xx}-2i\sigma_{xy}=2\{z\overline{\Phi'(z)}+\overline{\Psi(z)}\}$$
$$-2G_0\left(\frac{\partial^2\omega}{\partial x^2}-\frac{\partial^2\omega}{\partial y^2}+2i\frac{\partial^2\omega}{\partial x\partial y}\right) \quad (12)$$
$$2G_0(U'_{xx}/c+iU'_{yy}/c)=\kappa\Phi(z)-\overline{\Phi(z)}$$
$$-z\overline{\Phi'(z)}-\overline{\Psi(z)}+2G_0\left(\frac{\partial^2\omega}{\partial x^2}+i\frac{\partial^2\omega}{\partial x\partial y}\right) \quad (13)$$
$$\nabla^2\omega=\frac{1+\nu}{1-\nu}\alpha_0 T(x, y), \quad (14)$$

where primes denote differentiation with respect to $z(=x+yi)$ and $\nabla^2=\partial^2/\partial x^2+\partial^2/\partial y^2$, $\kappa=3-4\nu$.

First, consider the thermoelastic problem of a rigid roller sliding with friction and arbitrarily

NII-Electronic Library Service

The Japan Society of Mechanical Engineers

distributed heat input on an uncracked half-space. The quasi-stationary temperature solution in a half-space due to a fast-moving heat source, which satisfies the boundary conditions Eqs. (2) and (3), is given as[17]

$$T(x,y)=\begin{cases}0 & -\infty<x<-1\\ \dfrac{T^*}{\sqrt{\pi P_e}}\displaystyle\int_{-1}^{x}\frac{Q(t)}{\sqrt{x-t}}e^{-P_e^2y/4(x-t)}dt, & -1<x<1\\ \dfrac{T^*}{\sqrt{\pi P_e}}\displaystyle\int_{-1}^{1}\frac{Q(t)}{\sqrt{x-t}}e^{-P_e^2y/4(x-t)}dt, & 1<x<\infty,\end{cases} \tag{15}$$

where $T^*=2fVS_rP_0c/K_t$. Substituting Eq. (15) into Eq. (14), we can easily get the solution of ω. From the known solution for thermoelastic stress and displacement, the solution to this contact problem may be obtained by application of the methods described by Muskhelishvili[16] to the boundary conditions Eqs. (4)-(7). This procedure leads immediately to the Hilbert problem, the solution of which is[9]

$$\begin{aligned}\Phi_1(z)=&2iG_0(1+if)\{z-2\gamma-X(z)\}/\{R(\kappa+1)\}\\&+fS_rH_0P_rG_0\Big[\frac{-2i(1+if)\cos(\pi\gamma)}{\pi(\kappa+1)}S_0(z)\\&+\frac{\cos(\pi\gamma)}{\pi^2}\int_{-1}^{1}\Big\{Q(u)-\frac{f}{\sqrt{\pi P_e}}\hat{Q}_1(u)\Big\}S_1(z;u)du\\&+\frac{i}{2\pi\sqrt{\pi P_e}}\int_1^{\infty}\frac{S_3(v)}{v-z}dv\Big],\end{aligned} \tag{16}$$

where

$$S_0(z)=\int_{-1}^{1}\frac{Q(t)}{X^+(t)}\Big\{1+\frac{X(z)}{t-z}\Big\}dt \tag{17}$$

$$S_1(z;u)=\int_{-1}^{1}\frac{1}{X^+(t)(t-u)}\Big\{1+\frac{X(z)}{t-z}\Big\}dt,\ |u|<1 \tag{18}$$

$$S_3(v)=\int_{-1}^{1}Q(t)(t-v)^{-3/2}dt,\ 1\leqq v\leqq\infty \tag{19}$$

$$X^+(t)=(1+t)^{0.5-\gamma}(1-t)^{0.5+\gamma} \tag{20}$$

$$X(z)=(z+1)^{0.5-\gamma}(z-1)^{0.5+\gamma} \tag{21}$$

$$\gamma=\frac{1}{\pi}\tan^{-1}\frac{(\kappa-1)f}{\kappa+1} \tag{22}$$

$$\hat{Q}_1(u)=\frac{\partial}{\partial u}\int_{-1}^{u}\frac{Q(\varepsilon)}{(u-\varepsilon)^{1/2}}d\varepsilon. \tag{23}$$

The stresses and displacements in an uncracked half-space are given as follows[16].

$$\begin{aligned}(\sigma_{yy}-i\sigma_{xy})_{\Phi_1}=&\Phi_1(z)-\Phi_1(\bar{z})\\&+(z-\bar{z})\overline{\Phi_1'(z)}-2G_0\Big(\frac{\partial^2\omega}{\partial x^2}+i\frac{\partial^2\omega}{\partial x\partial y}\Big)\end{aligned} \tag{24}$$

$$\begin{aligned}2G_0(U_{xx}'/c+iU_{yy}'/c)_{\Phi_1}=&\kappa\Phi_1(z)+\Phi_1(\bar{z})\\&-(z-\bar{z})\overline{\Phi_1'(z)}+2G_0\Big(\frac{\partial^2\omega}{\partial x^2}+i\frac{\partial^2\omega}{\partial x\partial y}\Big)\end{aligned} \tag{25}$$

To account for the stress field caused by the crack, we consider the problem of a dislocation present at the point $z=z_0(z_0=x_1+iy_1+\eta e^{-i\beta})$ in an infinite space. Then the dislocation density is defined as

$$\alpha=\frac{G_0\{[U_{\xi\xi}]+i[U_{\xi\zeta}]\}e^{-i\beta}}{i\pi c(\kappa+1)} \tag{26}$$

where $\{[U_{\xi\xi}]+i[U_{\xi\zeta}]\}$ represents the displacement jumps. This problem is solved using the following complex potential functions[18].

$$\Phi_2(z)=\frac{\alpha}{z-z_0} \tag{27}$$

$$\Psi_2(z)=\frac{\bar{\alpha}}{z-z_0}+\frac{\alpha\bar{z}_0}{(z-z_0)^2} \tag{28}$$

Then the stress representation is given by Eqs. (11)-(13), and is $\omega=0$. An additional potential Φ_3, which is required to remove the surface tractions, is conveniently written in terms of Φ_2, Ψ_2 as[16]

$$\Phi_3(z)=\begin{cases}-\bar{\Phi}_2(z)-z\bar{\Phi}_2'(z)-\bar{\Psi}_2(z), & \mathrm{Im}(z)<0\\ \Phi_2(z), & \mathrm{Im}(z)>0.\end{cases} \tag{29}$$

Then the stress representation is given by Eqs. (24) and (25), and is $\omega=0$.

The superposition of the thermoelastic contact solution (Φ_1) on the dislocation solution (Φ_2, Ψ_2 and Φ_3) does not satisfy the boundary condition Eq. (6). In order to satisfy the surface boundary conditions Eqs. (4)-(6), an additional potential must be determined in order to remove the displacement effects beneath the roller that arise due to the dislocation. This interaction potential Φ_4 was derived by Bryant et al.[2], and their result can be expressed as

$$\begin{aligned}\Phi_4(z)=&-(1+if)/2[(\alpha+\bar{\alpha})\{F(z;z_0)-F(z;\bar{z}_0)\}\\&-(z_0-\bar{z}_0)\{\bar{\alpha}G(z;\bar{z}_0)+\alpha G(z;z_0)\}\\&+(\alpha+\bar{\alpha})\{1/X(z_0)-1/X(\bar{z}_0)\}\\&+(z_0-\bar{z})\{\bar{\alpha}X'(\bar{z}_0)/X^2(\bar{z}_0)\\&+\alpha X'(z_0)/X^2(z_0)\}],\end{aligned} \tag{30}$$

where

$$F(z;z_0)=\{1-X(z)/X(z_0)\}/(z-z_0) \tag{31}$$

$$G(z;z_0)=\{F(z;z_0)+X(z)X'(z_0)/X^2(z_0)\}/(z-z_0). \tag{32}$$

Thus, using the potentials Φ_j ($j=2,3,4$) and Ψ_2, we can obtain the stress field for a dislocation α. Replacing the constant α with distributed dislocation density $\alpha(\eta)d\eta$ defined along the line ξ of a subsurface crack, the stress due to the cracks can be obtained by integration of η.

Superposing these results with the thermoelastic roller solution (Φ_1), the stress solution which satisfies the boundary conditions Eqs. (2)-(7), can be obtained. With substitution of these stresses into Eqs. (8), (9) and (10), the following singular integral equations for α are obtained:

$$\begin{aligned}&2e^{i\beta}\int_0^{\iota}\frac{\alpha(\eta)}{\xi-\eta}d\eta+\int_0^{\iota}\{\alpha(\eta)F_1(\xi,\eta)\\&+\overline{\alpha(\eta)}F_2(\xi,\eta)\}d\eta\\&=-\{(\sigma_{\zeta\zeta}-i\sigma_{\xi\zeta})_{\Phi_1}\}_{\zeta=0}\end{aligned} \tag{33}$$

$$\int_0^{\iota}\alpha(\eta)d\eta=0 \tag{34}$$

where

$$\begin{aligned}F_1(\xi,\eta)=&\sum_{r=3}^{4}[\hat{\Phi}_r(z;z_0)+(1-e^{2i\beta})\overline{\Phi_r^*(z;z_0)}\\&-e^{2i\beta}\hat{\Phi}_r(\bar{z};z_0)+e^{2i\beta}(z-\bar{z})\overline{\Phi_r^{*\prime}(z;z_0)}]\end{aligned} \tag{35}$$

NII-Electronic Library Service

The Japan Society of Mechanical Engineers

$$F_2(\xi,\eta)=\sum_{r=3}^{4}[\hat{\Phi}_r^*(z;z_0)+(1-e^{2i\beta})\overline{\hat{\Phi}_r(z;z_0)} - e^{2i\beta}\Phi_r^*(\bar{z};z_0)+e^{2i\beta}(z-\bar{z})\overline{\hat{\Phi}_r'(z;z_0)}] \quad (36)$$

$$\hat{\Phi}_4(z;z_0)=-(1+if)/2\{F\{z;z_0)-F(z;\bar{z}_0) -(z_0-\bar{z}_0)G(z;z_0)+1/X(z_0)-1/X(\bar{z}_0) +(z_0-\bar{z}_0)X'(z_0)/X^2(z_0)\} \quad (37)$$

$$\Phi_4^*(z;z_0)=-(1+if)/2\{F\{z;z_0)-F(z;\bar{z}_0) -(z_0-\bar{z}_0)G(z;\bar{z}_0)+1/X(z_0)-1/X(\bar{z}_0) +(z_0-\bar{z}_0)X'(\bar{z}_0)/X^2(\bar{z}_0)\} \quad (38)$$

$$\hat{\Phi}_3(z;z_0)=\begin{cases}-1/(z-\bar{z}_0), & \mathrm{Im}(z)<0\\ 1/(z-z_0), & \mathrm{Im}(z)>0\end{cases} \quad (39)$$

$$\Phi_3^*(z;z_0)=\begin{cases}-(z_0-\bar{z}_0)/(z-z_0)^2, & \mathrm{Im}(z)<0\\ 0, & \mathrm{Im}(z)>0\end{cases} \quad (40)$$

$$z=x_1+iy_1+\xi e^{-2i\beta} \quad (41)$$

4. Numerical Calculations and Stress Intensity Factors

Equation (33), (34) was solved numerically using the piecewise quadratic method of Gerasoulis[19]. $a(\eta)$ is written as

$$a(\eta)=\frac{G_0\hat{a}(\hat{\eta})}{R(1-\hat{\eta}^2)^{1/2}}e^{-i\beta},\quad \hat{\eta}=2\eta c/\iota-1 \quad (42)$$

Let us divide the interval $[-1,1]$ into $2n$ equal parts. We define the nodal points as $\hat{\eta}_j=-1+(j-1)/n$ $(j=1\sim 2n+1)$, and use the Lagrange interpolation formula for three nodal points in the approximation. Setting the collocation points as $\xi_k=\eta_k+1/2n$ $(k=1\sim 2n)$, Eq. (33), (34) reduces to the simultaneous linear algebraic system of $(2n+1)$ equations for $a(\eta_j)$. Using these solutions, the stress intensity factors K_I^A, K_{II}^A at the crack tip A $(j=1)$ and K_I^B, K_{II}^B at the crack tip B $(j=2n+1)$ are given as

$$K_I^A-iK_{II}^A=-\frac{G_0}{R}\pi\sqrt{2c\iota}\,\hat{a}(-1) \quad (43)$$

$$K_I^B-iK_{II}^B=\frac{G_0}{R}\pi\sqrt{2c\iota}\,\hat{a}(1) \quad (44)$$

In carrying out the numerical calculations, it was necessary to determine iteratively the degree of crack opening for a given set of parameters. Iteration was performed under the condition of the absence of overlap of the material. First, the numerical solution was obtained for a completely open crack (ξ^{op}: $0<\xi<\iota$). The resulting crack opening displacement was checked by Eq. (26), and if overlap was found as $U_{\xi\xi}<0$, partial crack closure was approximated by setting $Re\{\hat{a}(\hat{\eta}_j)\}=0$ for that portion of the crack where overlap occurred. Then the procedure was repeated for the partially closed crack and results were verified. This method generally converged within three iterations. For the number of collocation points, a good accuracy was obtained for $n=10$.

Numerical calculations were carried out for the case of a short crack ($\iota=0.1$), and $P_e=100$ and $H_0=1.0$[20),(21)]. In Eq. (1), the heat input distribution $Q(x)$ is equal to the contact pressure distribution $P(x)=(\sigma_{yy})_{y=0}/P_0$. However, in the present analysis $P(x)$ is not given. Therefore, from the results of previous paper[14], $Q(x)$ is assumed to have a Hertzian distribution as

$$Q(x)=(1-x^2)^{1/2} \quad (45)$$

In the present numerical results, since the stress intensity factors at the both crack tips (A and B) are almost equal, we show the results only at the crack tip A. In the following, we represent K_I^A, K_{II}^A as K_I, K_{II}.

Figures 2 - 4 show the numerical results of stress intensity factors K_I, K_{II} as functions of the crack location over a complete loading cycle for the case of a horizontal crack ($\bar{\beta}=0°$) located at the depth $|y_1|=0.5$ for the various values of frictional coefficient f and slide/roll ratio S_r. From these figures, we can see that K_{II} attains a positive maximum at about $x_1=1$ which corresponds to the crack tip A being directly beneath the right edge of the contact region. Figure 2 shows the effects of frictional coefficient on the variation of K_I and K_{II} for $S_r=0.1$. The value of K_I and K_{II} increase with an increase of the frictional coefficient f. Figures 3 and 4 show the effects of slide/roll ratio S_r on the variation of K_I, K_{II} for $f=0.1$ and $f=0.7$ respectively. The value of K_I and K_{II} increase with an increase of the slide/roll ratio S_r peculiarly for large frictional coefficient as shown in Fig. 4. From these figures, we can see that the value of $(K_I)_{max}$ is so small that it may be disregarded as compared to the value of

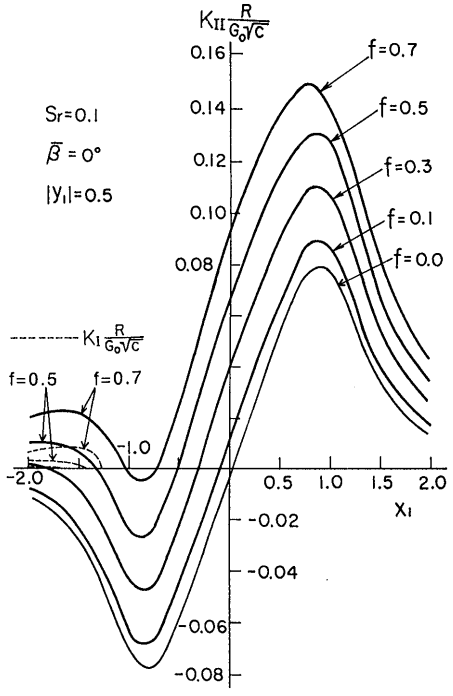

Fig. 2 Stress intensity factors as a function of crack location showing the effect of frictional coefficient f

NII-Electronic Library Service

The Japan Society of Mechanical Engineers

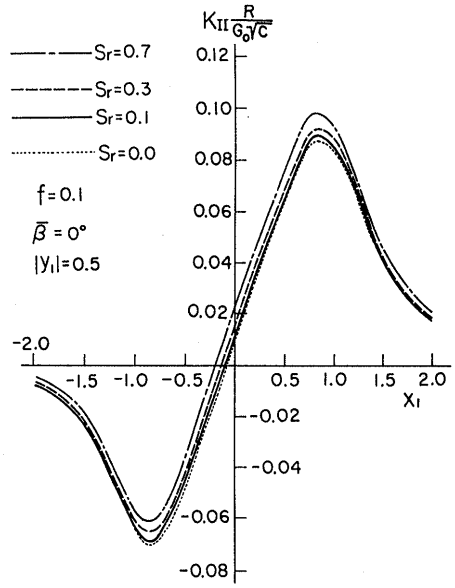

Fig. 3 Stress intensity factors as a function of crack location showing the effect of slide/roll ratio S_r for the case of $f=0.1$

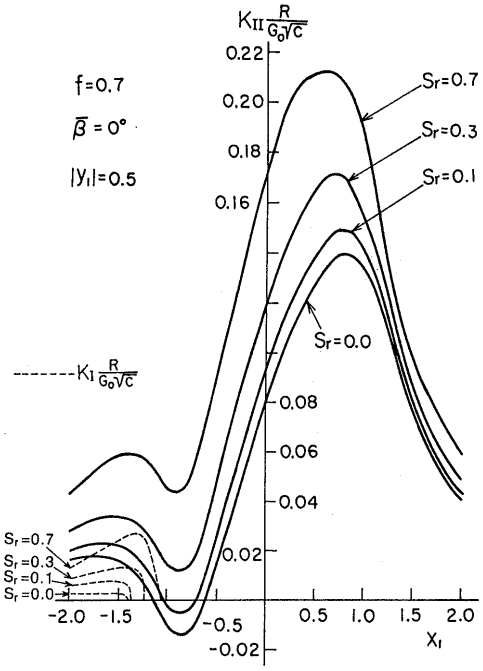

Fig. 4 Stress intensity factors as a function of crack location showing the effect of slide/roll ratio S_r for the case of $f=0.7$

$(K_{II})_{max}$. Therefore, the shearing mode crack growth seems to be predominant for the horizontal subsurface crack. The range of K_{II}, $\Delta K_{II}=(K_{II})_{max}-(K_{II})_{min}$, is the important quantity in fatigue considerations. For the case of $|y_1|=0.5$, the value of ΔK_{II} does not change very much with changing of the value of f and S_r as shown in Figs. 2 and 3.

In order to investigate the effects of crack depth $|y_1|$ on the stress intensity factors, Fig. 5 show the

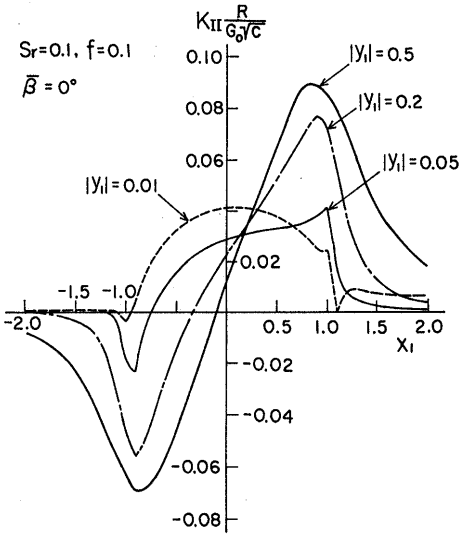

Fig. 5 Mode II Stress intensity factors K_{II} as a function of crack location showing the effect of subsurface crack depth $|y_1|$

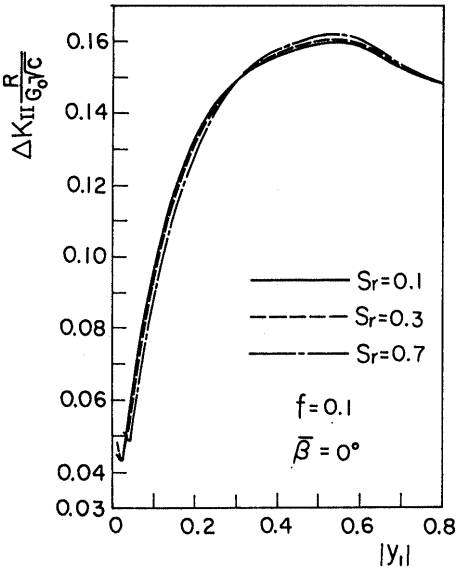

Fig. 6 $\Delta K_{II}=(K_{II})_{max}-(K_{II})_{min}$ as a function of subsurface crack depth $|y_1|$ for various slide/roll ratio S_r

variations of K_{II} as a function of horizontal crack location for changing the crack depth $|y_1|=0.5$, 0.2, 0.05, 0.01, for the case of $f=S_r=0.1$. As the crack approach the contact surface, the value of ΔK_{II} decreases and the variation of K_{II} become to be similar to the distribution of the contact pressure. Figure 6 shows ΔK_{II} as a function of horizontal crack depth $|y_1|$ for changing of the slide/roll ratio $R_s=0.1$, 0.3, 0.7, for the case of $f=0.1$. From this figure, we can see that ΔK_{II} attains a maximum at $|y_1|\fallingdotseq 0.5$ and ΔK_{II} decrease rapidly with a decrease of $|y_1|$. In this case, ΔK_{II} is not affected very much by the slide/roll ratio. Figure 7 shows ΔK_{II} as a function of horizontal crack depth $|y_1|$ for changing of the frictional coefficient

NII-Electronic Library Service

The Japan Society of Mechanical Engineers

f=0.1, 0.3, 0.5, 0.7, for the case of S_r=0.1. When $|y_1|<0.5$, as the crack approach the contact surface ΔK_{II} is significantly affected by the value of frictional coefficient. For example, when f=0.7 ΔK_{II} increases rapidly with a decrease of $|y_1|$. Therefore, when the frictional coefficient is small, the failure such as a shelling may occur at the depth $|y_1|\fallingdotseq 0.5$. However, for the case of large frictional coefficient (dry contact), it seems to be the most probable that the failure such as shelling occur at the vicinity of the contact surface. The numerical results in Figs. 6 and 7 are shown for the range of $|y_1|\geqq 0.01$ which is the limitation of the calculations.

Finally, in order to investigate the effects of the crack angle $\bar{\beta}$ on the stress intensity factors, Fig. 8 show the variations of K_{II} as a function of inclined crack location for changing the crack inclination angle $\bar{\beta}$= 0°, 10°, 50°, 90° for the case of $|y_1|$=0.5 and $f=S_r$=0.1. For the case of the horizontal or vertical crack, $|K_{II}|$ attain maximum at about x_1=1 which corresponds to the crack tip A being directly beneath the right edge of the contact region. For the case of $\bar{\beta}$=50°, K_{II} attain a negative maximum at x_1=0 which corresponds to the crack tip A being directly beneath the center of the contact region. Figure 9 shows ΔK_{II} as a function of $\bar{\beta}$ at three values of S_r for the case of $|y_1|$ =0.5 and f=0.1. From this figure, we can see that

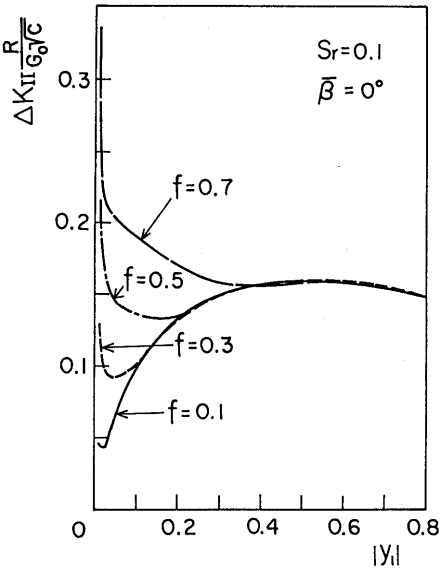

Fig. 7 $\Delta K_{II}=(K_{II})_{max}-(K_{II})_{min}$ as a function of subsurface crack depth $|y_1|$ for various frictional coefficients f

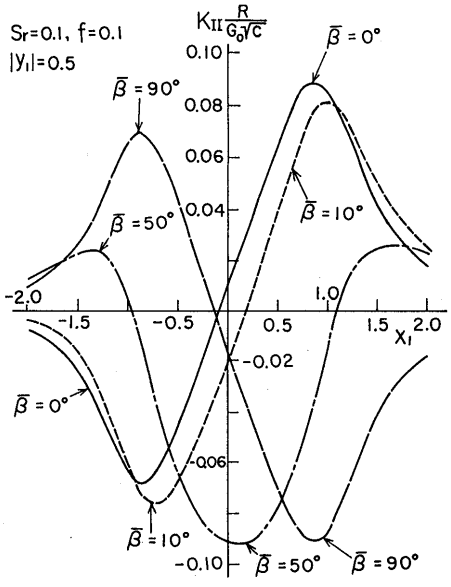

Fig. 8 Mode II Stress intensity factors K_{II} as a function of crack location showing the effect of inclined crack angle $\bar{\beta}$

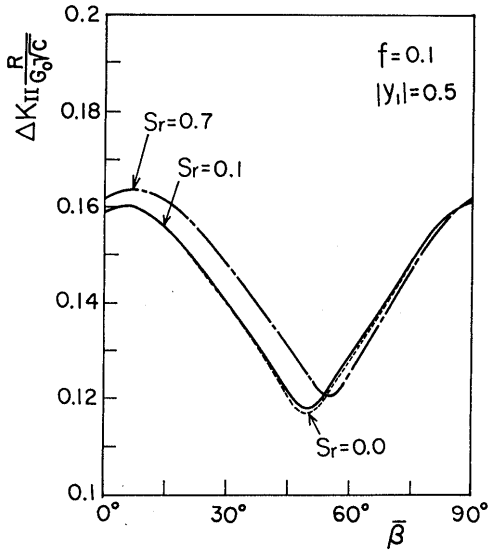

Fig. 9 $\Delta K_{II}=(K_{II})_{max}-(K_{II})_{min}$ as a function of the inclined crack angle $\bar{\beta}$ for various slide/roll ratio S_r

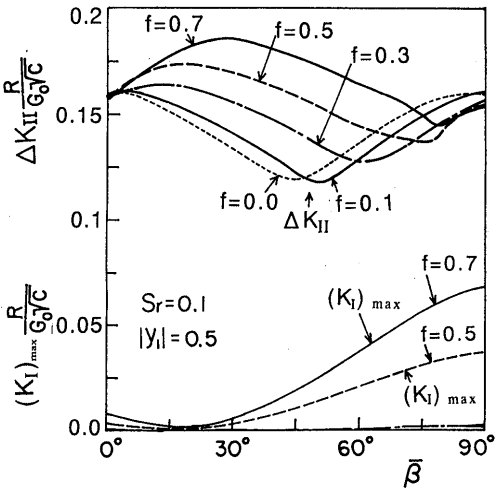

Fig. 10 $\Delta K_{II}=(K_{II})_{max}-(K_{II})_{min}$ as a function of the inclined crack angle $\bar{\beta}$ for various frictional coefficients f

NII-Electronic Library Service

The Japan Society of Mechanical Engineers

ΔK_{II} attains a maximum at $\bar{\beta} \fallingdotseq 7°$ or 90°, and ΔK_{II} shows a minimum at $\bar{\beta} \fallingdotseq 50°$. Figure 10 shows ΔK_{II} and $(K_I)_{max}$ as a function of $\bar{\beta}$ at five values of frictional coefficient f, for the case of $|y_1|=0.5$ and $S_r=0.1$. When the frictional coefficient is small, ΔK_{II} attains a maximum at the roughly horizontal or vertical crack. However, for the case of large frictional coefficient, ΔK_{II} attains a maximum at the inclined crack. For example, for the case of $f=0.7$ ΔK_{II} attains a maximum at $\bar{\beta} \fallingdotseq 30°$. $(K_I)_{max}$ increase with an increase of frictional coefficient and $(K_I)_{max}$ attains a maximum at $\bar{\beta} \fallingdotseq 90°$.

5. Conclusions

We analyzed the stress intensity factors for a subsurface crack due to rolling/sliding contact by a rigid roller with frictional heat generation. From numerical examples of the stress intensity factors for short cracks, the following conclusions can be drawn.

(1) The maximum values of stress intensity factors and ΔK_{II} increase with increasing of frictional coefficient and slide/roll ratio (increasing of thermal stresses).

(2) For small frictional coefficient, ΔK_{II} of horizontal subsurface crack attains a maximum when the subsurface crack depth is 1/2 of the half contact length. For large frictional coefficient, the value of ΔK_{II} increase as the subsurface crack approach to the contact surface.

(3) When the frictional coefficient is small, ΔK_{II} attains a maximum at $\bar{\beta} \fallingdotseq 0°$ or 90°, therefore the shear mode crack growth of the horizontal or vertical subsurface crack seems to be the most probable.

(4) When the frictional coefficient is large ($f=0.7$), ΔK_{II} attains a maximum at $\bar{\beta} \fallingdotseq 30°$, and $(K_I)_{max}$ attains a maximum at $\bar{\beta} \fallingdotseq 90°$, therefore the shear mode crack growth of the inclined subsurface crack or the mixed mode crack growth of the virtical subsurface crack seems to be the most probable.

Acknowledgment

The authors wish to thank Professor L.M. Keer of Northwestern University for his helpful suggestions.

References

(1) Suh, N.P., The Delamination Theory of Wear, Wear, Vol. 25 (1973), p. 111-124.

(2) Fleming, J.R. and Suh, N.P., Mechanics of Crack Propagation in Delamination Wear, Wear, Vol. 44 (1997), p. 39-56.

(3) Rosenfield, A.R., A Fracture Mechanics Approach to Wear, Wear, Vol. 61 (1980), p. 125-132.

(4) Hearle, A.D. and Johnson, K.L., Mode II Stress Intensity Factors for a Crack Parallel to the Surface of an Elastic Half-Space Subjected to a Moving Point Load, J. Mech. Phys. Solids, Vol. 33, No. 1 (1985), p. 61-81.

(5) Sheppard, S., Barber, J.R. and Comninou, M., Short Subsurface Cracks under Conditions of Slip and Stick Caused by a Moving Compressive Load, Trans. ASME, J. Appl. Mech., Vol. 52 (1985), p. 811-817.

(6) Miller, G.R., A Preliminary Analysis of Subsurface Crack Branching Under a Surface Compressive Load, Trans. ASME J. Tribol., Vol. 110 (1988), p. 292-297.

(7) Yu, M.M. and Keer, L.M., Growth of the Shell/Transverse Defect in Rails, Trans. ASME J. Tribol., Vol. 111 (1989), p. 648-654.

(8) Salehizadeh, H. and Saka, N., Crack Propagation in Rolling Line Contacts, Trans. ASME J. Tribol., Vol. 114 (1992), p. 690-697.

(9) Goshima, T. and Keer, L.M., Thermoelastic Contact Between a Rolling Rigid Indenter and a Damaged Elastic Body, Trans. ASME J. Tribol., Vol. 112 (1990), p. 382-391.

(10) Goshima, T., Hanson, M.T. and Keer, L.M., Three-Dimensional Analysis of Thermal Effects on Surface Crack Propagation in Rolling Contact, J. Thermal Stresses, Vol. 13 (1990), p. 237-260.

(11) Goshima, T. and Keer, L.M., Stress Intensity Factors of a Surface Crack in a Semi-Infinite Body due to Rolling-Sliding Contact and Frictional Heating, Trans. Jpn. Soc. Mech. Eng., (in Japanese), Vol. 56, No. 532, A (1990), p. 2567-2572.

(12) Goshima, T. and Miyao, K., Stress Intensity Factors of a Surface Crack in a Semi-Infinite Body due to Rolling-Sliding Contact and Transient Heating, Trans. Jpn. Soc. Mech. Eng., (in Japanese), Vol. 58, No. 547, A (1992), p. 393-399.

(13) Goshima, T. and Kamishima, Y., Mutual Interference of Multiple Surface Cracks Due to Rolling-Sliding Contact with Frictional Heating, JSME International J., Ser. A, Vol. 37, No. 3 (1994), p. 216-223.

(14) Goshima, T. and Kamishima, Y., Mutual Interference of Two Surface in a Semi-Infinite Body Due to Rolling Contact with Frictional Heating by a Rigid Roller, JSME International J., Ser. A, Vol. 39, No. 1 (1996), p. 26-33.

(15) Chen, T.Y. and Ju, F.D., High-Speed Frictional Heating of an Elastic Medium With a Near-Surface Horizontal Line Crack, Trans. ASME J. Tribol., Vol. 115 (1993), p. 56-60.

(16) Muskhelishvili, N.I., Some Basic Problems in the Mathematical Theory of Elasticity, (1954), 4th Ed. Noordhoff.

(17) Ling, F.F. and Mow, V.C., Surface Displacement of a Convective Elastic Half-Space Under an Arbitrarily Distributed Fast-Moving Heat Source, Trans. ASME J. Basic Eng., Vol. 87 (1965), p. 729-734.

(18) Dundurs, J., Mathematical Theory of Disloca-

NII-Electronic Library Service

The Japan Society of Mechanical Engineers

tions, (1975), p. 70, ASME Publication.
(19) Gerasoulis, A., The Use of Piecewise Quadratic Polynomials for the Solution of Singular Integral Equations of Cauchy Type, Comput. Math. Applics., Vol. 8 (1982), p. 15-22.
(20) Azarkhin, A., Barber, J.R. and Rolf, R.L., Combined Thermal-Mechanical Effects in Frictional Sliding, Key Engineering Materials, Vol. 33, (1989), p. 135-160.
(21) Hills, D.A. and Barber, J.R., Steady Motion of an Insulating Rigid Flat-Ended Punch Over a Thermally Conducting Half-Plane, Wear, Vol. 102 (1985), p. 15-22.

NII-Electronic Library Service